International Journal of GEOMATE, Oct., 2020, Vol.19, Issue 74, pp.98–106
ISSN: 2186-2982 (P), 2186-2990 (O), Japan, DOI: https://doi.org/10.21660/2020.74.55375
Geotechnique, Construction Materials and Environment

A PHYSICAL MODEL OF A GRAVITY WALL ON COMPACTED KHON KAEN LOESS

Worapong Phimonnok[1], *Ratamanee Nuntasarn[2], and Supakorn Tirapat[3]

[1,2,3] Faculty of Engineering, Khon Kaen University, Thailand

* Corresponding Author, Received: 25 April 2020, Revised: 14 May 2020, Accepted: 28 May 2020

ABSTRACT: This paper presents the testing of retaining walls on compacted Khon Kaen loess by using physical models. Khon Kaen loess was compacted in a box with the size 100 × 100 × 100 cm to achieve a dry density of 19 kN/cu.m, which was 90% of the maximum dry density of the modified method. Moreover, the moisture content of this compacted Khon Kaen loess was 11.85%. The effective friction angle (ϕ') and the effective cohesion (c') of this compacted Khon Kaen loess, as compacted, was 27 degrees and 12 kPa, respectively, using a direct shear test. The soil sample was compacted in five layers in the box, and the thickness of each layer was 45 cm. The dry density of each layer was examined using the sand cone method. A gravity wall 15 × 30 × 50 cm in size, was installed in the box to determine the stability of the retaining wall. An active force was applied using a pneumatic jack. The weight plate was applied to the top of the retaining wall as a vertical force. The horizontal and vertical movements were measured using LDVT. The passive force was measured using EPC at distances of 7, 10, 20, 32 and 45 cm from the retaining wall. The physical model indicates that passive force decreases with distance from the gravity wall. The physical modeling found that k_1 is 0.4, and k_2 is 0.5. The factor of safety against sliding and overturning should be larger than 1.5 and 2.5, respectively.

Keywords: Gravity Walls, Compacted Khon Kaen Loess, Physical Models, Passive Force, Active Force

1. INTRODUCTION

Khon Kaen loess is loose like a honeycomb, and it is classified as silty sand (SM) or clayey sand (SC). The sand grains may be bonded by clay silt or iron oxide (Fe2O3). As the moisture content increases, the bond between sand grains is destroyed. This causes the loss of shear strength, and it collapses suddenly.

Barden et al. [1] studied loess structure by collecting soil samples from around the world. Loess is predominantly sand, and clay particles or silt particles. Chemical cementing agents like calcium carbonate or iron oxide are the bonding agents. The collapse of loess can be attributed to three factors.

1. The structure is unsaturated and unstable, therefore easily destroyed.

2. Excessive stresses destroy the soil structure, causing subsidence.

3. An increase in moisture content dissolves the bonds and decreases the void ratio. This is a consequence of compact soil.

Collapsible soil is always found in arid and semi-arid areas. The soil in these climates is mostly unsaturated because of deep groundwater levels. The moisture content of the soil in the summer season is about 3%–5%; in the rainy season, it is about 10%–12%.

Udomchoke [2] found that the Khon Kaen loess is collapsible soil with a very severe degree of collapse. Moreover, the shear strength parameters of Khon Kaen loess decrease when the moisture content increases.

Gasaluck [3] found that loess covers many areas of northeastern Thailand. This loess has a relatively high permeability in which the soil's moisture content increases smoothly.

Muktabhant [4] indicated that the red color of the soil in Khon Kaen province, especially in Khon Kaen University, consist of fine sandy loam, silt, and clay. This is the causes of windblown as known as loess. The soil layer is about 4–8 meters thick. According to USCS, the Khon Kaen loess was classified as SM, SC, or SM-SC, with 13–19% of LL, 11–14% of PL, 0–5% of PI, and a specific gravity of 2.60–2.72.

M.R. Abdi [5] studied the pullout behavior of reinforcements using large pullout tests with a size of 100 × 60 × 60 cm and applied the load using a pneumatic jack.

Retaining walls are applied in engineering works such as embankments, excavation work, bridges, and waterproof structures to prevent the lateral movement of soil. Das [6] suggested the smallest dimension of the retaining wall, as shown in Fig. 1.

The failure mode of a retaining wall can be classified into four categories, as shown in Fig. 2: overturning, sliding, bearing capacity failure, and deep-seated shear failure. As the acting force on the retaining wall is shown in Fig.3, the safety factors

against overturning about the toe, sliding, and the bearing capacity are present in Eq. (1), Eq. (2) and Eq. (3), respectively. The minimum safety factors against overturning, sliding, and bearing capacity are 2, 1.5, and 3, respectively.

$$FS_{(overtruning)} = \frac{\sum M_R}{\sum M_O} \quad (1)$$

Where

$\sum M_R$ = sum of the moments resist overturn about point C

$\sum M_O$ = sum of the moments overturn about point C

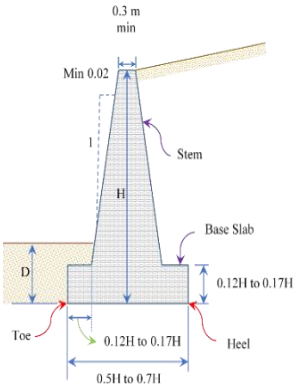

Fig.1 Smallest dimensions of the gravity retaining wall.

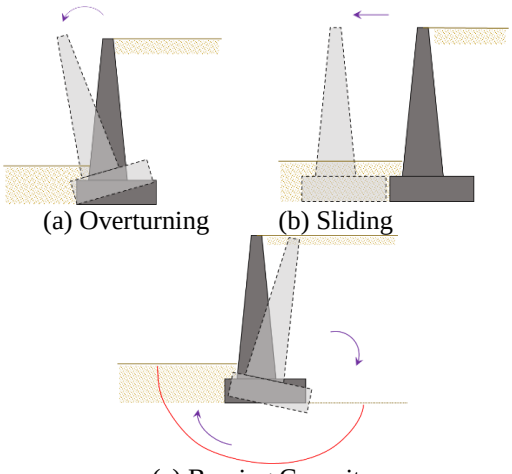

(a) Overturning (b) Sliding

(c) Bearing Capacity

Fig.2 Failure mode of the retaining wall.

$$FS_{(sliding)} = \frac{\sum F_{R'}}{\sum F_d} \quad (2)$$

Where

$\sum F_{R'}$ = sum of the horizontal resisting forces

$\sum F_d$ = sum of the horizontal driving forces

$$FS_{(\text{bearing capacity})} = \frac{q_u}{q_{\max}} \quad (3)$$

Where

q_u = ultimate bearing capacity

q_{max} = maximum pressure

At present, many projects are using Khon Kaen loess as backfill. Therefore, this study investigates the physical modeling of the retaining wall on compacted Khon Kaen loess. The Khon Kaen loess was compacted to 90% of the maximum dry density by the modified method on the wet side. Moreover, the gravity retaining wall is made of precast concrete.

2. APPARATUS

The modeling gravity retaining wall is 0.15 m wide, 0.50 m long and 0.30 m high.

The tank size is 1.0 × 1.0 × 1.0 m in width, length and depth, respectively.

The loading equipment (shown in Fig. 3) consists of:

(1) A pneumatic system that controls the horizontal active force using a 1 mm/min speed.

(2) A proving ring used to measure the horizontal active force.

(3) Four LDVTs used to determine vertical and horizontal displacements.

(4) Weight plates that were used as vertical loading.

(5) Two Earth Cell Pressure transducers (EPC) that were used to measure the passive pressure.

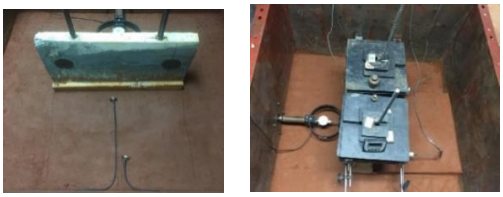

(a) Pressure Transducers (b) Weight Plates

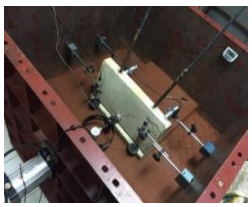

(c) Proving Ring, LDVTs and Pneumatics

Fig.3 Apparatus of Physical Model

3. METHODOLOGY

Khon Kaen loess was used to determine the basic classifying properties, according to [7].

Moreover, the Soil-Water Characteristic Curve (SWCC) was examined from the pressure plate [8]. The soil structure and chemical analysis were determined using a Scanning Electron Microscope (SEM) and an EDX, respectively. Moreover, the shear strength parameters were investigated using a direct shear test under an unconsolidated undrained test as a compacted condition [9]. The samples for SEM, EDX, direct shear test, and modeling were prepared to a compaction of 90% wet side of maximum dry density through modified compaction. Three vertical loads were applied to the retaining wall's physical model at 1.0, 2.0, and 4.0 kN.

3.1 Physical Model Test

The gravity wall model was 0.15 m width, 0.5 m long, and 0.3 m height. The depth of the gravity wall (D), as shown in Fig. 1, was 0.07 m. The test procedures are the following:

Step I: The Khon Kaen loess was compacted at the wet side of the optimum moisture content in the tank to achieve 90% maximum dry density. The soil sample was compacted in five layers, each of which was 9 cm thick. The dry density was then checked using the sand cone method.

Fig.4 This is how the soil sample was prepared.

Step II: Earth Pressure Cells (EPC) were installed 3 cm below the surface at distances of 10, 20, 32, and 45 cm from the gravity wall.

Step III: The speed of the pneumatic jack was adjusted to 1 mm/min to shear as shown in Fig.5.

Step IV: Four LDVTs were attached and adjusted to the gravity wall to measure a vertical and a horizontal displacement as shown in Fig.6.

Step V: The vertical loads were applied at the top of the modeling as shown in Fig.6.

Step VI: The pneumatic jack was started and initial shear.

Step VII: A vertical and horizontal displacement, active force, and passive force were recorded every 5 sec by using a data logger.

Step VIII: The test was terminated after the wall lifting.

4. RESULTS AND DISCUSSION

This part is divided into four sections. The first section presents the basic properties. The soil-water characteristic curve is discussed in the second section. The third part reveals the shear strength parameters of compacted Khon Kaen loess as a condition prepared by doing a direct shear test. The result of the physical model is presented in the final section.

4.1 Basic Properties

As shown in Table 1, the sieve analysis and hydrometer analysis reveal that the predominant material of Khon Kaen loess is sand, with silt and clay as the binders. In addition, Khon Kaen loess was classified as silty sand (SM) according to [10]. Moreover, the EDX's result, as presented in Table 2, showed a high percentage of iron, which can also be the binder of Khon Kaen loess. The comparison between the disturbed and the undisturbed Khon Kaen loess is shown in Fig.9. There are various sizes of the void in both samples. But there are numerous voids in an undisturbed sample compared to a disturbed one. Moreover, the structure of the undisturbed sample is flocculated, while the structure of the disturbed one is dispersed.

Fig.5 The adjustment of the pneumatic

4.2 Soil-Water Characteristic Curve

The soil sample was compacted in a mold to achieve a dry density of 19 kN/m^3 and the initial moisture content of 11.5%. Then, the mold, 5 cm in diameter and height, was compressed into the soil sample. The test result of the Soil-Water Characteristic Curve (SWCC) was shown in Fig. 8. There are two air-entry values and two residual points. The first and second air-entry values are 3 and 450 kPa, respectively. Moreover, the first and second residual degrees of saturation str 42% and 16%, respectively.

Fig.6 Test running

Table 1 Basic properties of Khon Kean loess.

Properties	
Liquid limit (LL) %	16.5
Plastic limit (PL) %	NP
Plasticity index (PI) %	-
Specific gravity	2.65
Optimum moisture content (OMC), %	7.22
Maximum dry density (γ_d), t/m^3	2.12
Sand (%)	55
Silt (%)	30
Clay (%)	15
USCS classification	SM

Table 2 EDXs of Khon Kaen loess

Element	Weight%	Atomic%	
O K	60.16	59.37	SiO_2
Na K	0.10	0.10	Albite
Mg K	0.06	0.06	MgO
Al K	8.74	8.62	Al_2O_3
Si K	25.93	25.59	SiO_2
K K	0.09	0.09	MAD-10 Feldspar
Ca K	0.09	0.09	Wollastonite
Ti K	0.69	0.69	Ti
Fe K	4.15	4.09	Fe
Totals	100.00		

4.3 Direct Shear Test (UU test)

Using the same preparation as the SWCC sample, Khon Kaen loess was compacted into a mold and then trimmed in the shear box. The initial dry density and moisture content was 19 kN/m^3 and 11.85%, respectively. The shear strength, c, and ϕ, were investigated using direct shear tests under unconsolidated, undrained, and without saturation. Fig. 9 illustrated the test results, with the total cohesion and friction angle of 12 kPa and 27 deg, respectively.

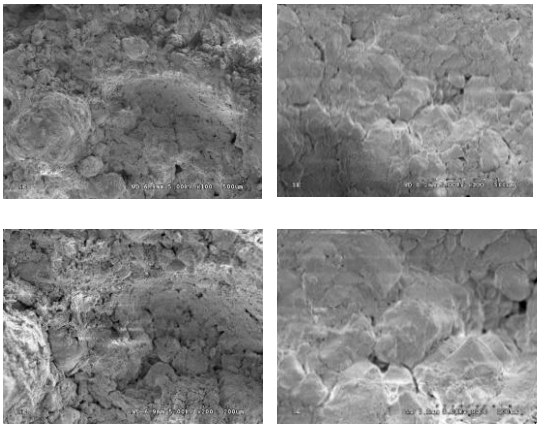

(a) Undisturbed Sample (b) Disturbed Sample

Fig.7 Khon Kaen loess structure in an undisturbed and disturbed condition

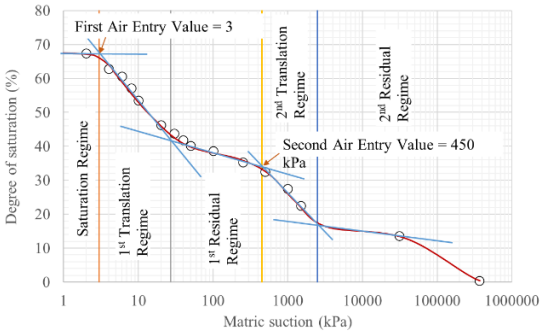

Fig.8 The soil-water characteristic curve (SWCC)

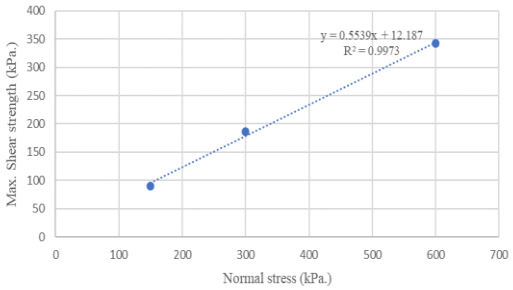

Fig.9 This is the result of a direct shear.

4.4 Physical Model Test

Three vertical loads of 1.0, 2.0, and 4.0 kN were applied at the top of the gravity wall as a multi-stage test. The applied active force was read out from the proving ring, while the passive force was displayed from the cell pressure installed in the soil sample at a depth of 3 cm from the ground surface. The differential active and passive forces were given as T-force. The relationship between the T-force and the horizontal displacement, as shown from Figs.10 to 14, revealed that T-force increased with the distance. This increase implied that the passive

force decreased with the distance, as shown in Fig.15.

The connection between T-force and vertical displacement, as shown from Figs.16 to 20, determined the uplifted point, going to the overturning of the gravity wall. This point was defined as the failure of sliding and overturning. T-forces at the failure were provided from Tables 3 to 7.

The relationships between the vertical and horizontal displacement as present in Figs.21 to 25 shown the dilation behavior of the sample.

The diagram containing the T-force of the failure and the normal force (N) at various distances of passive measurement can be seen in Fig.26 . The relationship between the T-force and the normal force can be expressed in Eq. (4).

$$T = c_d + m.N \tag{4}$$

Where c_d = y-intercept
m = the slope of the graph

The friction between the gravity wall and the soil beneath was represented by the kinetic friction (F_k) due to the sliding of the gravity wall with a constant rate of 1mm/min.

Whereas

$$F_k = \mu_k.N \tag{5}$$

Therefore, the slope of the graph (m) in Eq. (4) is μ_k, which is equal to $\tan\delta_k$. Eq. (4) can be written as

$$T = c_d + \tan(\delta'_k).\ N \tag{6}$$

Moreover, Eq. (6) also corresponds to the Mohr-Coulomb failure equation, as shown in Eq. (10).

$$\tau = c + \sigma.\tan\phi \tag{7}$$

Therefore, T, c_d and δ'_k are the shear force, the cohesion and the friction angle between the gravity wall and the soil beneath, respectively.

The ratio between c_d:c as k_1 and δ'_k:ϕ as k_2, as provided in Table 8, suggests that k_1 and k_2 should be 0.4 and 0.5, respectively, for the design gravity wall against the sliding failure.

Tables 9 and 10 show the safety factors against sliding and overturning, respectively. They were less than 1.5 and 2.5, as calculated in eq. (8) and (9), respectively. Therefore, the sliding and overturning safety factors must be greater than those values.

$$FS_{slidng} = \frac{P_p + F_k}{P_a} \tag{8}$$

$$FS_{overturning} = \frac{N\left(b/2\right)}{P_a\left(h/2\right)} \tag{9}$$

where N = normal force
b = width of the gravity wall
h = height of the gravity wall

Furthermore, Fig.27 shows that the passive failure is 13 cm from the gravity wall and the failure angle (θ) of 31 deg, as shown in Fig. 28. According to [11] the passive failure planes are (45-ϕ/2), whereas the friction angle (ϕ) of compacted Khon Kaen loess was 27 deg from direct shear test. That shows a good agreement. Moreover, the maximum horizontal movement was 0.07 m or 15.9% strain at failure, as shown in Fig.29.

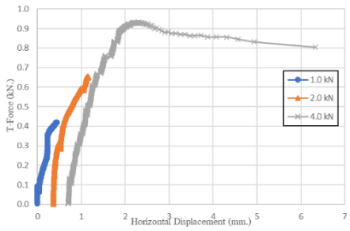

Fig.10 The relationship between the T-force and the horizontal displacement (EPC at 7 cm)

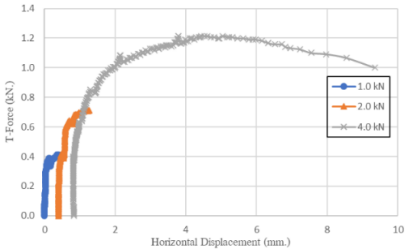

Fig.11 The relationship between the T-force and the horizontal displacement (EPC at 10 cm)

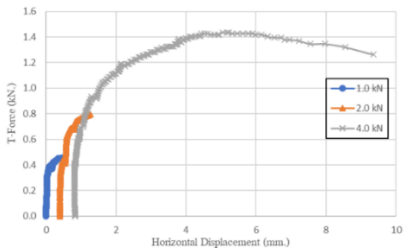

Fig.12 The relationship between the T-force and the horizontal displacement (EPC at 20 cm)

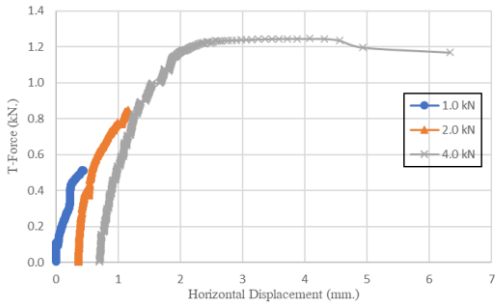

Fig.13 The relationship between the T-force and the horizontal displacement (EPC at 32 cm)

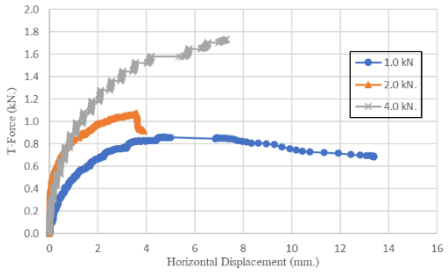

Fig.14 The relationship between the T-force and the horizontal displacement (EPC at 45 cm)

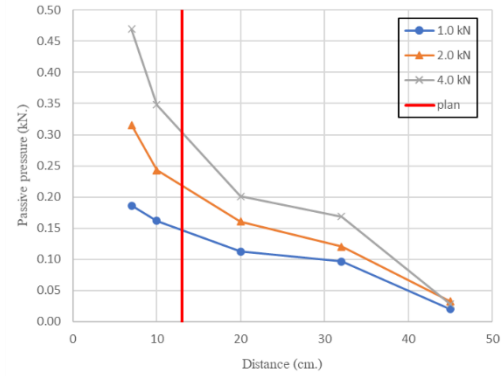

Fig.15 The relationship between passive pressure and distance of soil pressure transducers

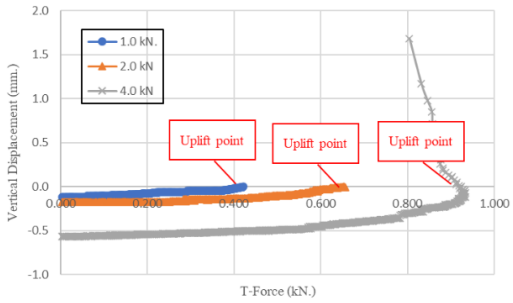

Fig.16 The relationship between the T-force and the vertical displacement (EPC at 7 cm)

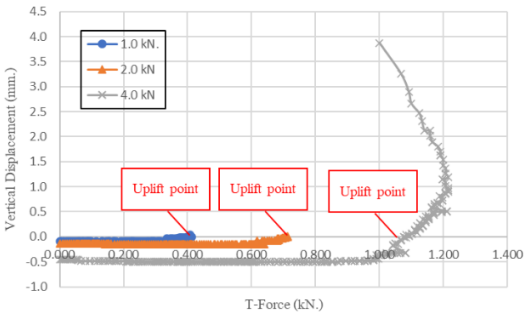

Fig.17 The relationship between the T-force and the vertical displacement (EPC at 10 cm.)

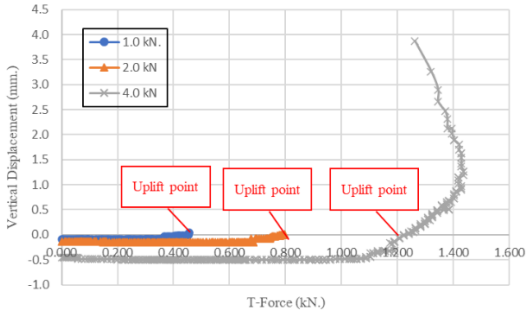

Fig.18 The relationship between the T-force and the vertical displacement (EPC at 20cm.)

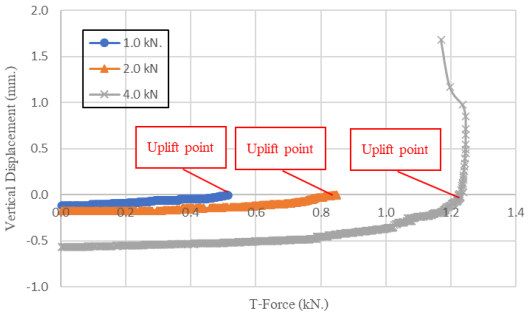

Fig.19 The relationship between the T-force and the vertical displacement (EPC at 32 cm)

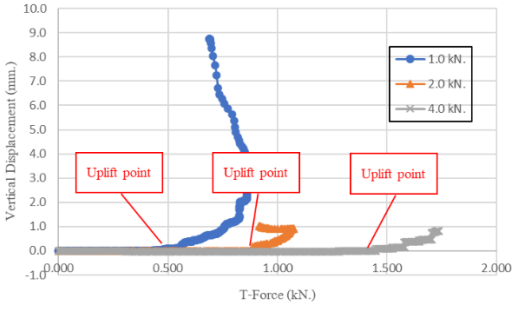

Fig.20 The relationship between the T-force and the vertical displacement (EPC at 45 cm.)

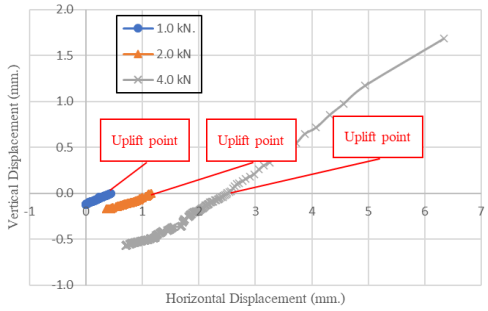

Fig.21 The relationship between the vertical displacement and the horizontal displacement (EPC at 7 cm.)

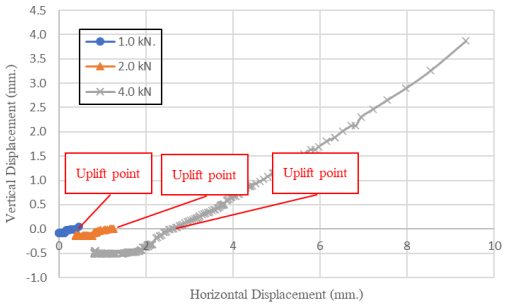

Fig.22 The relationship between the vertical displacement and the horizontal displacement (EPC at 10 cm.)

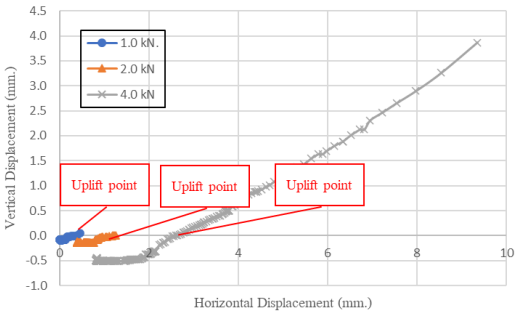

Fig.23 The relationship between the vertical displacement and the horizontal displacement (EPC at 20 cm.)

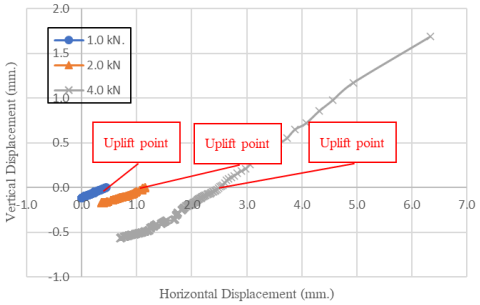

Fig.24 The relationship between the vertical displacement and the horizontal displacement (EPC at 32 cm.)

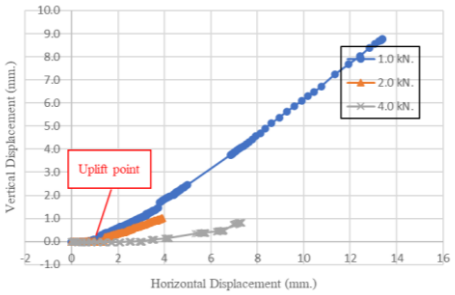

Fig.25 The relationship between the vertical displacement and the horizontal displacement (EPC at 45 cm.)

Table 3 The result at failure of EPC at 7 cm

P_v kN	σ_v kPa	P_a kN	P_p7 kN	T7 kN
1.0	13.08	0.607	0.186	0.421
2.0	26.16	0.969	0.316	0.653
4.0	52.32	1.394	0.470	0.924

Table 4 The result at failure of EPC at 10 cm

P_v kN	σ_v kPa	P_a kN	P_p10 kN	T10 kN
1.0	13.08	0.569	0.162	0.407
2.0	26.16	0.957	0.243	0.714
4.0	52.32	1.441	0.348	1.093

Table 5 The result at failure of EPC at 20 cm

P_v kN	σ_v kPa	P_a kN	P_p20 kN	T20 kN
1.0	13.08	0.569	0.113	0.457
2.0	26.16	0.957	0.161	0.796
4.0	52.32	1.441	0.201	1.240

Table 6 The result at failure of EPC at 32 cm

P_v kN	σ_v kPa	P_a kN	P_p32 kN	T32 kN
1.0	13.08	0.607	0.096	0.510
2.0	26.16	0.969	0.121	0.849
4.0	52.32	1.394	0.169	1.225

Table 7 The result at failure of EPC at 45 cm

P_v kN	σ_v kPa	P_a kN	P_p45 kN	T45 kN
1.0	13.08	0.584	0.020	0.564
2.0	26.16	0.930	0.032	0.897
4.0	52.32	1.390	0.028	1.362

Table 8 The coefficient (k_1 and k_2) of the cohesion and friction angle

Dist. cm.	c_d kN	δ'_k Deg	$k_1 = c'_d/c$	$k_2 = \delta/\phi$
7	0.391	14.16	0.428	0.489
10	0.324	15.73	0.354	0.543
20	0.324	15.79	0.355	0.545
32	0.392	14.27	0.429	0.493
45	0.354	14.73	0.387	0.508

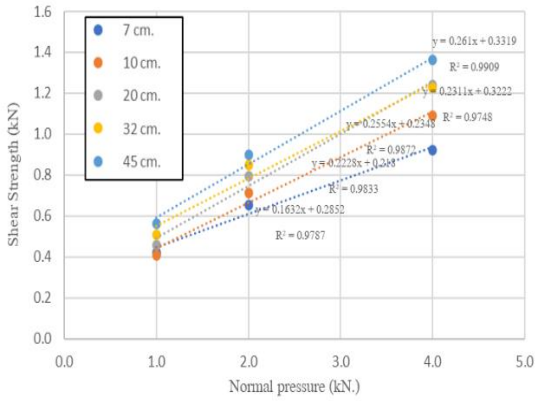

Fig.26 The relationship between the normal pressure (N) and the T-force

Table 9 The factor of safety against sliding

Distanc cm.	$FS_{sliding}$ $P_v = 1.0$	$P_v = 2.0$	$P_v = 4.0$
7	1.367	1.250	1.133
10	1.348	1.181	1.248
20	1.264	1.098	1.149
32	1.225	1.054	1.133
45	1.090	0.981	1.031

Table 10 The factor of safety against overturning

Distsnce cm.	$FS_{overturning}$ $P_v = 1.0$	$P_v = 2.0$	$P_v = 4.0$
7	1.236	1.548	2.152
10	1.317	1.568	2.082
20	1.317	1.568	2.082
32	1.236	1.548	2.152
45	1.284	1.614	2.159

Fig.27 Failure plane

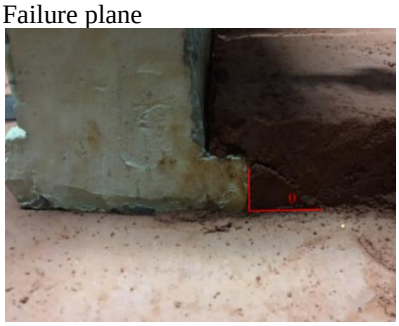

Fig.28 Passive plane failure

Fig.29 Horizontal movement

5. CONCLUSION

The predominant component of Khon Kaen loess is sand; silt, clay, and iron oxide are the binders. The structure of the undisturbed sample is flocculated, while the structure of the disturbed sample is dispersed. The SWCC of compacted Khon Kaen loess indicates the bimodal mode, which means the pore size of compacted Khon Kaen loess varies. The total cohesion and friction angle of the prepared condition is 27 deg and 12 kPa, respectively, by direct shear test under unconsolidated and undrained methods without a

saturation stage. Moreover, the physical model indicates that passive pressure decreases with distance from the gravity wall. The physical modeling found that k_1 is 0.4, and k_2 is 0.5. The failure plane is 13 cm from the gravity wall, which is agreed to [11] according to direct shear result. The factor of safety against sliding and overturning should be larger than 1.5 and 2.5, respectively.

6. ACKNOWLEDGMENT

Acknowledgment is given to the Sustainable Infrastructure Research and Development Center (SIRDC), Khon Kaen University, for supporting this research.

7. REFERENCES

[1] Barden L., McGown A., and Collins K., he collapse mechanism in partly saturated soil. Engineer Geology 1973 February, pp.305-317.

[2] Udomchoke V., Origin and Engineering Characteristics of the Problem Soil in the Khorat Basin, Northeastern Thailand, Ph.D. dissertation, Asian Institute of Technology, Bangkok, Thailand, 1991.

[3] Gasaluck W., Influence of moisture content on bearing capacity of Khon Kaen loess, the 5th National Convention on Civil Engineering, Pattaya, Thailand, 1999.

[4] Muktabhant C., Soil Mechanics, Khon Kaen University–1st edition, Khon Kaen, Thailand, 2009.

[5] Abdi M.R., and Zandieh A.R., Experimental and numerical analysis of large-scale pull-out tests conducted on clays reinforced with geogrids encapsulated with coarse material, Geotextiles and Geomembranes 42, 2014, pp.494-504.

[6] Das B.M., Principles of Foundation Engineering–7th edition, 2011.

[7] American Society for Testing and Materials (D422-63), Standard Test Method for Particle-Size Analysis of Soils.

[8] Perez-Garcia N., Houston S., Houston W., and Padilla J., An Oedometer-Type Pressure Plate SWCC Apparatus, Geotechnical Testing Journal 31, No. 2, 2008, pp.115-123.

[9] Takada N., Mikasa's Direct Shear Apparatus, Test Procedures and Results, Geotechnical Testing Journal 16, No. 3, 1993, pp.314-322.

[10] American Society for Testing and Materials (D2487-98), Standard practice for classification of soils for engineering purposes (Unified Soil Classification System).

[11] Rankine W., On the stability of loose earth, Philosophical Transactions of the Royal Society of London, Vol. 147, 1856.